

Phosphoglycolate phosphatase is a metabolic proof-reading enzyme essential for cellular function in
Plasmodium berghei

Lakshmeesha Kempaiah Nagappa¹, Pardhasaradhi Satha², Thimmaiah Govindaraju², Hemalatha Balam¹

From the ¹Molecular Biology and Genetics Unit and ²Bioorganic Chemistry Laboratory, New Chemistry Unit, Jawaharlal Nehru Centre for Advanced Scientific Research (JNCASR), Bengaluru, Karnataka, INDIA.

Running title: *P. berghei* phosphoglycolate phosphatase

To whom correspondence should be addressed: Hemalatha Balam, Molecular Biology and Genetics Unit, Jawaharlal Nehru Centre for Advanced Scientific Research (JNCASR), Jakkur P.O., Bengaluru, Karnataka, 560064, India. Tel: 91-80-22082812 Fax: 91-80-22082766. E-mail:hb@jncasr.ac.in

Keywords: *Plasmodium berghei*, phosphoglycolate phosphatase (PGP), 2-phosphoglycolate, 2-phospho L-lactate, 4-phosphoerythronate

ABSTRACT

Plasmodium falciparum (Pf) 4-nitrophenylphosphatase has previously been shown to be involved in vitamin B1 metabolism. Here, conducting a BLASTP search, we found that 4-nitrophenylphosphatase from Pf has significant homology with phosphoglycolate phosphatase (PGP) from mouse, human, and yeast, prompting us to reinvestigate the biochemical properties of the *Plasmodium* enzyme. Because the recombinant Pf PGP enzyme is insoluble, we performed an extended substrate screen and extensive biochemical characterization of the recombinantly expressed and purified homolog from *Plasmodium berghei* (Pb), leading to the identification of 2-phosphoglycolate and 2-phospho-L-lactate as the relevant physiological substrates of Pb PGP. 2-Phosphoglycolate is generated during repair of damaged DNA ends, 2-phospho-L-lactate is a product of pyruvate kinase side reaction, and both potently inhibit two key glycolytic enzymes, triosephosphate isomerase and phosphofructokinase. Hence, PGP-mediated clearance of these toxic metabolites is vital for cell survival and functioning. Our results differ significantly from those in a previous study wherein the Pf PGP enzyme has been inferred to act on 2-phospho-D-lactate and not on the L isomer. Apart from resolving the substrate specificity conflict through direct *in vitro*

enzyme assays, we conducted PGP gene-knockout studies in *P. berghei*, confirming that this conserved metabolic proof-reading enzyme is essential in *Plasmodium*. In summary, our findings establish Pb PGP as an essential enzyme for normal physiological function in *P. berghei* and suggest that drugs that specifically inhibit *Plasmodium* PGP may hold promise for use in anti-malarial therapies.

Haloacid dehalogenase superfamily (HADSf) is a large family of enzymes consisting mainly of phosphatases and phosphotransferases, that are both intracellular and extracellular in nature. These enzymes are characterized by the presence of a core Rossmannoid-fold and a cap-domain (1, 2). Studies on HADSf members have focused on identifying their physiological substrates by screening a wide range of metabolites that include sugar phosphates, lipid phosphates, nucleotides as well as phosphorylated amino acids and co-factors. This approach has helped understand the physiological relevance of these enzymes in various cellular processes such as cell wall synthesis, catabolic and anabolic pathways, salvage pathways, signaling pathways and detoxification (3–13). Apart from dephosphorylating metabolites, HADSf members have also been known to dephosphorylate proteins and such members are characterized by the absence of the cap

domain (1, 2). A large scale study reported by Huang *et al.*, has identified a HADSF member from *Salmonella enterica* that catalyzes dephosphorylation of more than 100 phosphorylated substrates (5). This extended substrate specificity is a common observation in HADSF members and often leads to a confounding situation where determining the physiological substrate of such promiscuous enzymes becomes a challenging task.

Recent studies have identified and characterised HADSF members from the apicomplexan parasite, *Plasmodium* (4, 10, 13–16). HADSF members from *Plasmodium* have been found to be involved in processes that lead to the development of resistance to the drug fosmidomycin, which inhibits isoprenoid biosynthesis (4). Also, these enzymes show considerable activity towards nucleotide monophosphates and phosphorylated co-factors, and generic substrates such as p-nitrophenylphosphate (pNPP) and β -glycerophosphate. A HADSF member that was annotated as 4-nitrophenylphosphatase from *P. falciparum* (gene id. PF3D7_0715000) was characterized by Knöckel *et al.*, (2008) and was proposed to be involved in dephosphorylation of thiamine monophosphate, the precursor of the active form of vitamin B1 (thiamine pyrophosphate). *In vitro* assays on the purified recombinant enzyme showed that this protein displayed similar specific activities towards thiamine monophosphate and other substrates (ADP, ATP, CTP, G-6-P, F-6-P and PLP) (15). An independent BLASTp search conducted by us revealed that this protein sequence has significant homology (28-30 %) with phosphoglycolate phosphatase (PGP) from yeast, human and mouse (Fig. 1). The (His)₆-tagged recombinant *P. falciparum* (Pf) 4-nitrophenylphosphatase when expressed in *Escherichia coli*, was found to be completely insoluble. However, *P. berghei* (Pb) 4-nitrophenylphosphatase (gene id. PBANKA_1421300) (referred to as PbPGP hereonwards) that shares 69.6 % identity (Fig. 1B) with its *Pf* homolog, expressed in the soluble form in *E. coli* and could be purified to homogeneity. Here, we report on the biochemical characterization and essentiality of PbPGP. An extended substrate screen identified 2-phosphoglycolate and 2-phospho L-lactate as relevant physiological sub-

strates in addition to the generic substrates pNPP and β -glycerophosphate. Attempts at gene ablation showed that PbPGP gene cannot be disrupted in *P. berghei*, despite the loci being non-refractory for genetic recombination. Our findings emphasize the importance of the ‘metabolic proof-reading’ process, which involves clearance or modification of toxic cellular metabolites generated as a consequence of error in substrate recognition by enzymes of intermediary metabolism. This process is universal and is analogous to the DNA proof-reading observed in polymerases and aminoacyl-tRNA synthetases (17). Our studies on PbPGP establish the essential physiological nature and biochemical function of this conserved cytosolic enzyme, and suggest that drugs that specifically inhibit parasite phosphoglycolate phosphatase can be promising anti-malarial agents.

RESULTS

Biochemical characterization of recombinant PbPGP — BLASTp analysis of Pf and Pb PGP protein sequences showed 28-30 % sequence homology with phosphoglycolate phosphatase, a conserved protein, present across eukaryotes from yeast to mouse including humans, involved in metabolic proof-reading (Fig. 1A). The Pf and Pb protein sequences show 69.6 % identity (Fig. 1B).

Upon expression of C-terminal (His)₆-tagged PfPGP in Rosetta DE3 pLysS strain of *E. coli*, the protein was found to be present completely in the insoluble fraction (Fig. S1A). This was unlike the strep-tagged PfPGP that was reported to be present in small quantities in the soluble fraction and hence amenable to purification. Therefore, we made use of the protein solubility prediction software PROSOII and found that homologues of PfPGP from other Plasmodia were predicted to be soluble (Fig. S1B). Hence, the previously uncharacterized *P. berghei* homolog was chosen for further biochemical studies and physiological investigations. PbPGP was expressed in the *E. coli* strain Rosetta DE3 pLysS and purified to homogeneity by Ni-NTA affinity chromatography (Fig. S1C) followed by size-exclusion chromatography (Fig. 2A).

PbPGP on analytical gel filtration using Sephacryl S-200 column showed a mass of about

78 kDa, whereas the theoretical mass is 37 kDa, indicating that the protein is a dimer (Fig. 2B and C). When further analyzed in the presence of 1 M NaCl, there was a shift in oligomeric state of the protein from dimer, towards monomer suggesting that the oligomers are held by electrostatic interactions (Fig. 2B and C).

A total of 38 compounds were screened as possible substrates for PbPGP. Although the enzyme displayed very low activity towards nucleotides and sugar phosphates as reported for PfPGP by Knöckel *et al.*, (15) a novel observation was made as a consequence of our extended substrate screen. PbPGP showed very high activity on 2-phosphoglycolate and 2-phospho L-lactate in addition to the generic substrates pNPP and β -glycerophosphate (Fig. 2D). It should be noted that the enzyme was stereospecific for 2-phospho L-lactate and showed no activity on 2-phospho D-lactate.

Kinetic studies on PbPGP—PbPGP showed maximum activity at pH 7.0 and preferred Mg^{2+} as co-factor over other divalent cations (Fig. 3B and C). The substrate saturation plots for β -glycerophosphate, 2-phosphoglycolate and 2-phospho L-lactate were hyperbolic (Fig. 3D-F) and were fit to Michaelis-Menten equation to obtain the kinetic parameters such as K_m and V_{max} (Table 1). PbPGP has higher K_m value for 2-phosphoglycolate (3.3 and 11.4 fold) and 2-phospho L-lactate (27.4 and 6.4 fold) when compared with that of murine PGP and yeast Pho13. The k_{cat} value for PbPGP for 2-phosphoglycolate is 11.4 and 3.9 fold higher and for 2-phospho L-lactate is 37 and 8.9 fold higher when compared to that of murine and yeast homologs, respectively. The catalytic efficiency (k_{cat}/K_m) for 2-phosphoglycolate was 3.5 fold higher and 2.9 fold lower when compared with its murine and yeast homologs respectively. With 2-phospho L-lactate as substrate, the parasite enzyme has similar catalytic efficiency as its murine and yeast homologs.

Probing the essentiality of PbPGP and localization in P. berghei—pJAZZ linear knockout vector for PbPGP was generated by following the strategy described by Pfander *et al.*, (18). Drug resistant parasites were not obtained in the first transfection attempt. In the second attempt, though drug

resistant parasites were obtained, genotyping by PCR revealed non-specific integration of the marker cassette. These parasites were positive by PCR for both the PbPGP gene and the hDHFR marker but were negative for specific 5' and 3' integration PCRs (Fig. S4). Since it was not possible to obtain knockout parasites, a conditional knockdown (at the protein level) strategy was employed by tagging the gene for PbPGP with a regulatable fluorescent affinity tag (RFA) where stability of the fusion protein is conditional to the binding of the small molecule trimethoprim. The conditional knockdown vector was also generated by following the recombineering strategy and validated by PCR (Fig. 4). Transgenic parasites were obtained in the first transfection attempt itself and genotyping by PCR showed the presence of a single homogenous population with correct insertion of RFA tag (Fig. 4F). Nevertheless, it was observed that the reduction in the levels of RFA-tagged protein upon removal of TMP, varied between 30-60 % across experiments and complete knockdown could not be achieved (Fig. 5A-C). As a consequence, there was no significant difference in growth rate between parasites grown in mice fed with or without trimethoprim (Fig. 5D and E).

The transgenic RFA-tagged *P. berghei* parasites were employed to determine localization of PbPGP and upon microscopic observation a cytosolic GFP signal was observed in all the intraerythrocytic stages (Fig. 5F).

DISCUSSION

Earlier Knöckel *et al.*, had performed a TBLASTN search and identified a potential 4-nitrophenylphosphatase in *P. falciparum*. The authors had proposed a novel role for this HADSF member and suggested involvement in vitamin B1 homeostasis (15). We found the *P. falciparum* 4-nitrophenylphosphatase sequence to have homology with human, mouse and yeast phosphoglycolate phosphatases. An extended substrate specificity screen of the recombinant *P. berghei* enzyme revealed that, indeed this protein is phosphoglycolate phosphatase, which is mainly involved in detoxification, having very high activity on 2-phosphoglycolate and 2-phospho L-lactate with no activity on thiamine monophosphate. 2-

phosphoglycolate is reported to be formed during repair of free radical mediated damage of DNA ends (19) and accumulation of this metabolite in the cell, leads to inhibition of the key glycolytic enzyme triosephosphate isomerase (TIM) (Fig. 6). Studies on phosphoglycolic acid phosphatases from yeast and mouse have demonstrated that this enzyme also performs metabolic proof-reading by catabolizing the substrates 2-phospho L-lactate and 4-phosphoerythronate which are products of enzymatic side reactions. Activity of PbPGP on 4-phosphoerythronate could not be tested due to non availability of the compound. 2-phospho L-lactate, generated by phosphorylation of L-lactate by pyruvate kinase, is known to inhibit phosphofructokinase and 4-phosphoerythronate, which is a product of GAPDH side reaction, is known to inhibit 6-phosphogluconate dehydrogenase (Fig. 6) (20). Due to the detrimental effect of these metabolites, it becomes essential to clear the cell of these metabolic toxins. This is reflected upon by the fact that phosphoglycolate phosphatase is an essential gene in mouse (21). Also, in *Arabidopsis*, knockout of PGLP1 isoform leads to impaired post-germination development of primary leaves (22).

Plasmodium in its intra-erythrocytic stages experiences very high levels of oxidative stress (23) leading to an increased ROS production that can damage its DNA, the repair of which will result in generation and accumulation of 2-phosphoglycolate. The parasite performs lactic acid fermentation and secretes large amounts of lactate into the medium, most of which is L-lactate (93-94 %), in addition to a small proportion of D-lactate (6-7 %) that is known to be produced through the methylglyoxal pathway (24). This lactate can accumulate and be phosphorylated in the cell to give rise to 2-phospholactate. In a recent study, Dumont *et al.*, through metabolite profiling of wild type and Δpfp *P. falciparum* concluded that PfPGP has specificity for 2-phospho D-lactate while our studies contradict this inference and provide direct evidence for the sole substrate specificity for the L-isomer. In their experiment, Δpfp parasites when grown under normal culture conditions or in the presence of 2 mM L-lactate showed a similar 12 fold higher accumulation of phospholactate when compared with wildtype parasites grown un-

der the same culture conditions. However, in the presence of increasing concentrations of D-lactate in the culture medium, they observed a dose dependent increase in the accumulation of phospholactate that is not significantly different between wild type and Δpfp parasites. Although this rules out the absence of PfPGP activity being the cause for 2-phospho D-lactate accumulation, the authors have concluded that PfPGP utilizes 2-phospho D-lactate as a substrate (16). The physiological reasons for these observations of Dumont *et al.*, can be rationalized in the following manner. As L-lactate is the predominant isomer produced in high concentrations in the cell, externally added L-lactate may not be taken up inside the cell or even if taken up, might not significantly perturb intracellular L-lactate concentration. Therefore, in the experiment of Dumont *et al.*, addition of L-lactate to the culture medium did not lead to an increase in levels of phospholactate in wild type or Δpfp parasites (16). Whereas, D-lactate is produced in the parasite at very low levels and exogenously added D-lactate might be acted upon by pyruvate kinase to form 2-phospho D-lactate. This can happen in both wild type and Δpfp parasites and the absence of significant difference in levels of phospholactate accumulation between wild type and Δpfp parasites when grown in the presence of D-lactate (16) is expected as our studies show that PGP is specific for only 2-phospho L-lactate. Further, Dumont *et al.*, perform metabolite profiling of wt and $\Delta glo1$ (impaired in D-lactate production) parasites in the presence of methyl glyoxal in the culture medium and observe similar levels of phospholactate accumulation in both parasites. The authors justify this observation by speculating that either methyl glyoxal is converted to D-lactate by RBC and then transported to the parasite or is directly converted to D-lactate in the parasite by the involvement of apicoplast glyoxalase-1 (16). Either way, D-lactate levels in the parasite increase, gets phosphorylated and accumulates in both wildtype and $\Delta glo1$ parasites as phospholactate, in spite of the presence of PGP gene. This again goes to show that PGP does not act on the D-isomer. As pyruvate kinase is known to have higher binding affinity for D-lactate when compared to that for L-lactate (25), accumulation of phospholactate in wildtype and Δpfp

parasites grown on D-lactate and parasites grown on methyl glyoxal could be a consequence of preferential activity of pyruvate kinase on D-lactate. The indirect inferences provided by Dumont *et al.*, are akin to a 'phenocopy' witnessed as a consequence of pyruvate kinase activity on D-lactate, rather than a true phenotype associated with phosphoglycolate phosphatase deficiency. Our results on the purified enzyme directly show that PbPGP acts only on 2-phospho L-lactate and not on 2-phospho D-lactate (Fig. 2D). We further validated this by performing enzyme assays with 1 mM 2-phospho L-lactate in the presence or absence of 10 mM 2-phospho D-lactate. The absence of significant change in specific activity clearly shows that 2-phospho D-lactate does not bind to the enzyme (Fig. 3A). This observation is consistent with that of the murine homolog of PbPGP that also acts only on 2-phospho L-lactate (20). In addition to the above evidences, the possible difference in substrate specificity across the enzymes from the two *Plasmodium* species, *P. falciparum* and *P. berghei* was also addressed by taking recourse to sequence and structural analysis of the proteins. Both proteins are highly identical and residues around the four HAD motifs are highly conserved (Fig. S5A). Both protein sequences were subjected to homology modeling and both modeled structures aligned without any gross structural differences (Fig. S5B and C). This strongly suggests that PfPGP like PbPGP would also have specificity for only 2-phospho L-lactate.

Recombinant human pyruvate kinase M2 isoform has been shown to phosphorylate L-lactate leading to the production of 2-phospho L-lactate that was in turn, shown to inhibit phosphofructokinase-2 activity in crude lysates of HCT116 cells and activity of recombinant phosphofructokinase-fructose 1,6-bisphosphatase (PFKFB) isozymes, PFKFB3 and PFKFB4 (20). Interestingly, in yeast, knockout of PHO13 (PGP homolog) is viable as yeast performs alcohol fermentation instead of lactate fermentation and hence does not accumulate phospholactate. Also, the inhibition of pentose-phosphate pathway caused by accumulation of 4-phospho D-erythronate is countered by transcriptional up-regulation of pentose-phosphate pathway enzymes (20). *Plasmodium* has two genes coding for phosphofructokinase, one on

chromosome 9 (PfPFK9) and the other on 11 (PfPFK11) and only PfPFK9 has been shown to be functional. It has been reported that unlike the host enzyme, PfPFK9 lacks regulation by fructose 1,6-bisphosphate, phosphoenolpyruvate and citrate (26). In such a scenario, we speculate that 2-phospho L-lactate might directly inhibit PfPFK9 to regulate glycolysis as knockout of PbPGP is not possible. This selective mode of regulation might be unique to *Plasmodium*.

In *Plasmodium*, where glycolysis is the sole source of ATP in asexual stages (27), the parasite cannot afford inhibition of its critical enzymes such as PFK and TIM arising from accumulation of toxic metabolites. Hence, having a metabolic proof-reading/detoxifying enzyme becomes vital for its survival. Inability to obtain knockout parasites indicates essentiality of this protein for parasite survival during asexual stages. To rule out the possibility of the loci being refractory for genetic recombination regulatable fluorescent affinity (RFA) tagging was attempted and a homogenous population of transfectants with RFA-tag integrated at the right loci was obtained. Having established that the loci is amenable for genetic manipulation, conditional knockdown strategy at protein level making use of the RFA tag (28) was adopted. Conditional knockdown at the protein level showed only 30-60 % reduction and hence parasites were viable (Fig. 5A-E). Similar observation has been described for yoelipain where the authors were neither able to knockout nor achieve significant knockdown of protein levels to see growth difference. Therefore, it was concluded that the gene was essential during intra-erythrocytic stages (29). Our results are similar and indicate essentiality of PbPGP in asexual stages. This conclusion on the gene essentiality of PbPGP is in agreement with the findings of Dumont *et al.*, on PfPGP where, $\Delta pfpgp$ parasites show growth defect (16). Further biochemical and structural studies on PGP could pave way for rational design of inhibitors with potent anti-malarial activity.

EXPERIMENTAL PROCEDURES

Materials—All chemicals, molecular biology reagents, and media components were from Sigma Aldrich, New England Biolabs, Gibco, In-

vitrogen and US biochemicals, USA; SRL, Spectrochem and Himedia, India. *E. coli* strain XL-1 blue, expression strain Rosetta (DE3) pLysS, and plasmids pET22b, and pET23d were from Novagen. The pJAZZ library clone (PbG02_B-53b06), plasmids pSC101BAD, R6K Zeo/pheS, and GW_R6K_GFP-mut3, and *E. coli* pir strains were procured from Plasmogem, Sanger Institute, UK. *E. coli* TSA cells were from Lucigen. Plasmid pGDB was a kind gift from Dr. Vasant Muralidharan, University of Georgia, USA. The *P. falciparum* 3D7 strain and *P. berghei* ANKA strain were procured from MR4. Amaxa 4D nucleofector and P5 Nucleofection kit were from Lonza, Germany. Gene sequencing of the various plasmid constructs was by Sanger sequencing method. Sequences of oligonucleotides used are provided in the section ‘Supplementary information’ (Table S1).

Bio-informatic analysis—PfPGP (PlasmogemDB gene ID PF3D7_0715000) protein sequence obtained from PlasmogemDB database was subjected to homology search against the non-redundant database at NCBI using the BLASTp algorithm. Clustal Omega (30) was used to generate multiple sequence alignment. ProsoII (31) was employed to predict solubility of proteins upon heterologous expression in *E. coli* system.

Cloning expression and purification of PfPGP and PbPGP—All expression plasmids with the desired gene of interest were generated in XL-1 blue strain of *E. coli* cells. Table S1 lists the oligonucleotide sequences used. PfPGP gene was amplified by PCR from *P. falciparum* genomic DNA using the primers P1 and P2. The purified PCR product was digested with restriction enzymes NcoI and XhoI and ligated with double digested plasmid pET23d. Chemically competent *E. coli* XL-1 blue cells were transformed with the ligation mix and transformants were selected on Luria-Bertani medium (LB) plates containing ampicillin ($100 \mu\text{g mL}^{-1}$) and tetracycline ($10 \mu\text{g mL}^{-1}$). The clones were validated by DNA sequencing. Plasmid isolated from the confirmed clone (pET23d_PfPGP) was used to transform Rosetta DE3 pLysS strain of *E. coli*.

Single colony of transformed Rosetta DE3 pLysS was inoculated into 10 mL of TB medium containing ampicillin ($100 \mu\text{g mL}^{-1}$) and chloram-

phenicol ($34 \mu\text{g mL}^{-1}$) and incubated at 37°C at 180 rpm for 12 - 15 hours. The overnight culture was inoculated (1 mL / 100 mL) into 800 mL TB containing ampicillin and chloramphenicol. The cells were allowed to grow at 37°C , 180 rpm till 0.6 OD₆₀₀ was reached and thereafter induced with IPTG at a final concentration of 0.3 mM. Induction was carried out at 18°C , 180 rpm for 15 hrs. The cells were harvested by centrifugation at $4000 \times g$ for 15 minutes at 4°C . The harvested cells were resuspended in 25 mL of lysis buffer (20 mM Tris HCl, pH 7.4, 100 mM NaCl, 1 mM DTT, 0.1 mM PMSF and 10 % w/v glycerol) and the cell suspension was lysed by passing through French pressure cell at 1000 psi for 7 cycles. The lysate was centrifuged at $18000 \times g$ for 30 minutes at 4°C . The supernatant was collected, mixed with 0.5 mL packed volume of Ni-NTA agarose beads and incubated at 4°C for 3 hours with rotation. The suspension was then transferred to a glass column and the flow through was collected. The beads were washed using lysis buffer containing increasing concentrations of imidazole. Pellet from centrifuged cell lysate, unbound (flow through), and wash fractions were analysed by 12 % SDS-PAGE and gel stained with Coomassie brilliant blue R-250.

PbPGP was amplified by PCR from *P. berghei* genomic DNA using the primers P3 and P4. The PCR product was cloned into pET22b between sites NdeI and XhoI. Cloning procedure and protocol for protein expression was similar to that of PfPGP. The fractions from Ni-NTA chromatography containing PbPGP were concentrated and subjected to further purification by size-exclusion chromatography on Sephacryl S-200 column (1.5 cm x 60 cm).

Determination of oligomeric state—Oligomeric state of PbPGP was determined by analytical size-exclusion chromatography using Sephacryl S-200 (1 cm x 30 cm) column attached to an AKTA Basic HPLC system. The column was equilibrated using 100 mM Tris HCl, pH 7.4 and 100 mM KCl at 0.8 mL min^{-1} flow rate and calibrated using the molecular weight standards; β -amylase (200 kDa), alcohol dehydrogenase (150 kDa), bovine serum albumin (66 kDa), carbonic anhydrase (29 kDa) and cytochrome C (12.4 kDa). $100 \mu\text{L}$ of PbPGP at 1 mg mL^{-1} concentration was

injected into the column and eluted with equilibration buffer with monitoring at 280 nm. The molecular mass of PbPGP was estimated by interpolating the elution volume on a plot of logarithm of molecular weight standards on the Y-axis and elution volume on the X-axis. Gel-filtration was performed with and without NaCl in the equilibration buffer.

Synthesis of 2-phospholactate—Synthesis of both D and L phospholactate was carried out following available procedure (20). The details of the protocol and characterization of the molecules are provided in ‘Supplementary information’ (Fig. S2 and S3).

Enzyme assays—A comprehensive substrate screen comprising of various classes of molecules such as, nucleoside phosphates, sugar phosphates, co-enzymes, amino acid phosphates, etc. was performed. The assay was carried out in 100 mM Tris HCl, pH 7.4, 2 mM substrate, 1 mM MgCl₂ in a volume of 100 μ L. The reaction mix was pre-incubated at 37 °C for 1 minute, the assay was initiated using 2 μ g enzyme and the reaction was allowed to proceed at 37 °C for 5 minutes. The reaction was stopped by the addition of 20 μ L of 70 % trichloroacetic acid (TCA) and 1 mL of freshly prepared Chen’s reagent (water, 6 N sulphuric acid, 2.5 % ammonium molybdate and 10 % L-ascorbic acid mixed in the ratio 2:1:1:1) was added, mixed thoroughly and incubated at 37 °C for 1.5 hours. The color developed was measured against blank (reaction mix to which enzyme was added after addition of TCA) at 820 nm. Specific activity was calculated using the ϵ value of 25000 M⁻¹ cm⁻¹.

pH optimum of PbPGP was determined by performing the assay in a mixed buffer containing 50 mM each of glycine, MES, Tris at different pH, 1 mM MgCl₂ and 1 mM pNPP as substrate in 100 μ L volume. The reaction mix was pre-incubated at 37 °C for 1 minute and the assay was initiated using 0.2 μ g enzyme and the reaction was allowed to proceed at 37 °C for 2 minutes, stopped using TCA and processed using Chen’s reagent as described above.

Preferred divalent metal ion was identified by using 10 mM pNPP as substrate and different salts such as MgCl₂, MnCl₂, CaCl₂, CuCl₂, and CoCl₂ at a final concentration of 1 mM in a 250 μ L reaction mix containing 50 mM Tris HCl, pH 8. The reaction was initiated with 0.26 μ g of en-

zyme and conversion of pNPP to p-nitrophenol was continuously monitored at 405 nm at 37 °C temperature. Slope of the initial 20 seconds of the progress curve was used to calculate specific activity using an ϵ value of 18000 M⁻¹ cm⁻¹.

Kinetic studies— K_m values for 2-phosphoglycolate, 2-phospho L-lactate and β -glycerophosphate was determined by measuring initial velocity at varying substrate concentrations ranging from 0.5 mM to 15 mM for 2-phosphoglycolate and 2-phospho L-lactate and 0.25 mM to 30 mM for β -glycerophosphate. The concentration of MgCl₂ was fixed at 5 mM with the reaction buffer being 200 mM Tricine-NaOH, pH 7.4. The reaction in a volume of 100 μ L was initiated with 1.89 μ g of enzyme, allowed to proceed at 37 °C for 2 minutes, stopped using TCA and processed using Chen’s reagent as described above. Specific activity was plotted as a function of substrate concentration and the data points were fitted to the Michaelis-Menten equation using GraphPad prism V5 to determine the kinetic parameters (32).

Generation of P. berghei transfection vectors—The library clone for *P. berghei* PGP (PbG02_B-53b06) was obtained from Plasmogem. The procedure for knockout and tagging construct generation was as described earlier (18, 33) and is provided in detail in ‘Supplementary information’.

Cultivation and transfection of P. berghei—Male/female BALB/c mice aged 6-8 weeks were used for cultivation and transfection of *P. berghei*. Glycerol stock of wild type *P. berghei* ANKA parasites was injected into a healthy male BALB/c mouse. The parasitemia was monitored by microscopic observation of Giemsa stained smears of blood drawn from tail snip. Transfection of the parasites was done by following the protocol described by Janse *et al.*, (34), using Amaxa 4D nucleofector (P5 solution and FP167 programme) followed by injection into 2 mice. For PbPGP knockout, drug resistant parasites were selected for by feeding infected mice with pyrimethamine in drinking water (7 mg in 100 mL), whereas parasites with PbPGP RFA-tag were selected for by feeding infected mice with trimethoprim in drinking water (30 mg in 100 mL). Drug resistant parasites were harvested in heparin solution (200 units mL⁻¹) made in RPMI-1640. Glycerol stocks were made

by mixing 300 μL of 30 % glycerol and 200 μL of the harvested blood and stored in liquid nitrogen. Validation of the drug resistant parasites was done by PCR.

Conditional knockdown of PbPGP in P. berghei—Glycerol stock of PbPGP RFA-tagged parasites was injected into a healthy BALB/c mouse. The parasitemia was monitored by microscopic observation of Giemsa stained smears of blood drawn from tail snip. Trimethoprim pressure was maintained throughout the growth period. Upon parasitemia reaching 5-10 %, about 500 μL of infected blood was collected in 500 μL of RPMI-1640 solution containing heparin. A 100 μL of this parasite containing suspension was injected into a fresh mouse that was fed with trimethoprim in drinking water and a second 100 μL to another mouse that was not fed with trimethoprim. Parasites were harvested from both mice after 6 days and subjected to Western blotting. The entire experiment was repeated twice.

Glycerol stock of PbPGP RFA-tagged *P. berghei* was injected into a healthy BALB/c mouse and parasitemia was monitored by Giemsa stained smears. Blood was harvested in heparin solution once parasitemia reached 0.5-1 % and 1.7×10^5 parasites were injected into two batches of mice (n=5). One batch was fed with drinking water containing trimethoprim (30 mg in 100 mL) and the other with water lacking trimethoprim. Parasitemia was monitored regularly starting from day 2 post-injection by counting parasites in Giemsa stained smears. Growth rate was determined by plotting percent-

age parasitemia on y - axis against time (number of days) on x - axis. Mortality rate among infected mice fed with/without trimethoprim containing water was also determined by plotting percentage survival of mice on y - axis against time (number of days) on x - axis.

Localization of PGP in P. berghei—PbPGP RFA-tagged parasites were harvested in heparin solution, centrifuged at $2100 \times g$ for 5 minutes and the supernatant discarded. The cells were resuspended in $1 \times \text{PBS}$ containing Hoeschst 33342 ($10 \mu\text{g mL}^{-1}$) and incubated at room temperature for 15 minutes. Thereafter, the cells were collected, washed once with $1 \times \text{PBS}$, resuspended in 70 % glycerol and dispersed on poly L-lysine coated cover slips that were mounted on glass slides, sealed and stored at 4 °C. The slides were observed under oil immersion objective (100 \times) of Zeiss LSM 510 Meta confocal microscope.

Ethics statement—Animal experiments involving handling of BALB/c mice were performed by adhering to standard procedures prescribed by the Committee for the Purpose of Control and Supervision of Experiments on Animals (CPCSEA), a statutory body under the Prevention of Cruelty to Animals Act of 1960 and Breeding and Experimentation Rules of 1998, Constitution of India. The current study (project no. HB006/201/CPCSEA) was approved by Institutional animal ethics committee (IAEC) of Jawaharlal Nehru Centre for Advanced Scientific Research that comes under the purview of CPCSEA.

Acknowledgments: This project was funded by; 1) Department of Biotechnology, Ministry of Science and Technology, Government of India. Grant number: BT/PR11294/BRB/10/1291/2014, BT/PR13760/COE/34/42/2015, and BT/INF/22/SP27679/2018. 2) Science and Engineering Research Board, Department of Science and Technology, Government of India. Grant number: EMR/2014/001276 and, 3) Institutional funding from Jawaharlal Nehru Centre of Advanced Scientific Research, Department of Science and Technology, India. LKN acknowledges CSIR for junior and senior research fellowships. TG acknowledges Department of Science and Technology, Government of India (Grant number: DST/SJF/CSA-02/2015-2016) for funding. PS acknowledges Science and Engineering Research Board, Department of Science and Technology, Government of India for post-doctoral fellowship (Grant number: 2017/000920). The authors thank Mr. Madhav Nayak for initial help in synthesis of phospholactate, Mrs. Suma for help in confocal microscopy and Dr. R. G. Prakash for help in animal handling.

Conflict of interest: The authors declare that they have no conflicts of interest with the contents of this

article.

Author contributions: HB and LKN conceived the project and designed the experiments. LKN performed biochemical and physiological characterization. PS synthesized and characterized 2-phospholactate under the supervision of TG. LKN and HB wrote the manuscript.

REFERENCES

1. Allen, K. N. and Dunaway-Mariano, D. (2004) Phosphoryl group transfer: evolution of a catalytic scaffold. *Trends Biochem. Sci.* **29**, 495–503
2. Allen, K. N. and Dunaway-Mariano, D. (2009) Markers of fitness in a successful enzyme superfamily. *Curr. Opin. Struct. Biol.* **19**, 658–665
3. Burroughs, A. M., Allen, K. N., Dunaway-Mariano, D., and Aravind, L. (2006) Evolutionary genomics of the had superfamily: understanding the structural adaptations and catalytic diversity in a superfamily of phosphoesterases and allied enzymes. *J. Mol. Biol.* **361**, 1003–1034
4. Guggisberg, A. M., Park, J., Edwards, R. L., Kelly, M. L., Hodge, D. M., Tolia, N. H., and Odom, A. R. (2014) A sugar phosphatase regulates the methylerythritol phosphate (MEP) pathway in malaria parasites. *Nat. Commun.* **5**, 4467
5. Huang, H., Pandya, C., Liu, C., Al-Obaidi, N. F., Wang, M., Zheng, L., Keating, S. T., Aono, M., Love, J. D., Evans, B., Seidel, R. D., Hillerich, B. S., Garforth, S. J., Almo, S. C., Mariano, P. S., et al. (2015) Panoramic view of a superfamily of phosphatases through substrate profiling. *Proc. Natl. Acad. Sci.* **112**, E1974–E1983
6. Kuznetsova, E., Proudfoot, M., Gonzalez, C. F., Brown, G., Omelchenko, M. V., Borozan, I., Carmel, L., Wolf, Y. I., Mori, H., Savchenko, A. V., Arrowsmith, C. H., Koonin, E. V., Edwards, A. M., Yakunin, A. F. (2006) Genome-wide analysis of substrate specificities of the *Escherichia coli* haloacid dehalogenase-like phosphatase family. *J. Biol. Chem.* **281**, 36149–36161
7. Kuznetsova, E., Nocek, B., Brown, G., Makarova, K. S., Flick, R., Wolf, Y. I., Khusnutdinova, A., Evdokimova, E., Jin, K., Tan, K., Hanson, A. D., Hasnain, G., Zallot, R., de Crécy-Lagard, V., Babu, M., et al. (2015) Functional diversity of haloacid dehalogenase superfamily phosphatases from *Saccharomyces cerevisiae* biochemical, structural, and evolutionary insights. *J. Biol. Chem.* **290**, 18678–18698
8. Proudfoot, M., Kuznetsova, E., Brown, G., Rao, N. N., Kitagawa, M., Mori, H., Savchenko, A., and Yakunin, A. F. (2004) General enzymatic screens identify three new nucleotidases in *Escherichia coli* biochemical characterization of sure, yfbr, and yjgg. *J. Biol. Chem.* **279**, 54687–54694
9. Roberts, A., Lee, S.-Y., McCullagh, E., Silversmith, R. E., and Wemmer, D. E. (2005) YbiV from *Escherichia coli* k12 is a HAD phosphatase. *Proteins: Struct. Funct. Bioinforma.* **58**, 790–801
10. Srinivasan, B., Nagappa, L. K., Shukla, A., and Balaram, H. (2015) Prediction of substrate specificity and preliminary kinetic characterization of the hypothetical protein PVX_123945 from *Plasmodium vivax*. *Exp. Parasitol.* **151**, 56–63
11. Titz, B., Häuser, R., Engelbrecher, A., and Uetz, P. (2007) The *Escherichia coli* protein YjgG is a house-cleaning nucleotidase in vivo. *FEMS Microbiol. Lett.* **270**, 49–57
12. Weiss, B. (2007) Yjgg, a dump phosphatase, is critical for thymine utilization by *Escherichia coli* k-12. *J. Bacteriol.* **189**, 2186–2189
13. Guggisberg, A., Frasse, P., Jezewski, A., Kafai, N., Gandhi, A., Erlinger, S., and Odom, A. J. (2018) Suppression of drug resistance reveals a genetic mechanism of metabolic plasticity in malaria parasites. *MBio* **9**, e01193-18
14. Srinivasan, B. and Balaram, H. (2007) ISN1 nucleotidases and had superfamily protein fold: *in silico* sequence and structure analysis. *In Silico Biol.* **7**, 187–193
15. Knöckel, J., Bergmann, B., Müller, I. B., Rathaur, S., Walter, R. D., and Wrenger, C. (2008) Filling the gap of intracellular dephosphorylation in the *Plasmodium falciparum* vitamin B1 biosynthesis. *Mol. Biochem. Parasitol.* **157**, 241–243
16. Dumont, L., Richardson, M. B., van der Peet, P., Dixon, M. W., Williams, S. J., McConville, M. J., Tilley, L., and Cobbold, S. (2018) The metabolic repair enzyme phosphoglycolate phosphatase regulates central carbon metabolism and fosmidomycin sensitivity in *Plasmodium falciparum*. *BioRxiv*, 415505
17. Van Schaftingen, E., Rzem, R., Marbaix, A., Collard, F., Veiga-da Cunha, M., and Linster,

- C. L. (2013) Metabolite proofreading, a neglected aspect of intermediary metabolism. *J. Inherit. Metab. Dis.* **36**, 427–434
18. Pfander, C., Anar, B., Schwach, F., Otto, T. D., Brochet, M., Volkmann, K., Quail, M. A., Pain, A., Rosen, B., Skarnes, W., Rayner, J. C., Billker, O. (2011) A scalable pipeline for highly effective genetic modification of a malaria parasite. *Nat. Methods* **8**, 1078
 19. Pellicer, M. T., Nunez, M. F., Aguilar, J., Badia, J., and Baldoma, L. (2003) Role of 2-phosphoglycolate phosphatase of *Escherichia coli* in metabolism of the 2-phosphoglycolate formed in DNA repair. *J. Bacteriol.* **185**, 5815–5821
 20. Collard, F., Baldin, F., Gerin, I., Bolsée, J., Noël, G., Graff, J., Veiga-da Cunha, M., Stroobant, V., Vertommen, D., Houddane, A., Rider, M. H., Linster, C. L., Van Schaftingen, E., Bommer, G. T. (2016) A conserved phosphatase destroys toxic glycolytic side products in mammals and yeast. *Nat. Chem. Biol.* **12**, 601–607
 21. Segerer, G., Hadamek, K., Zundler, M., Fekete, A., Seifried, A., Mueller, M. J., Koentgen, F., Gessler, M., Jeanclos, E., and Gohla, A. (2016) An essential developmental function for murine phosphoglycolate phosphatase in safeguarding cell proliferation. *Sci. Rep.* **6**, 35160
 22. Schwarte, S. and Bauwe, H. (2007) Identification of the photorespiratory 2-phosphoglycolate phosphatase, pglp1, in *Arabidopsis*. *Plant Physiol.* **144**, 1580–1586
 23. Atamna, H. and Ginsburg, H. (1993) Origin of reactive oxygen species in erythrocytes infected with *Plasmodium falciparum*. *Mol. Biochem. Parasitol.* **61**, 231–241
 24. Vander Jagt, D. L., Hunsaker, L. A., Campos, N. M., and Baack, B. R. (1990) D-lactate production in erythrocytes infected with *Plasmodium falciparum*. *Mol. Biochem. Parasitol.* **42**, 277–284
 25. Nowak, T. and Mildvan, A. S. (1972) Nuclear magnetic resonance studies of the function of potassium in the mechanism of pyruvate kinase. *Biochemistry* **11**, 2819–2828
 26. Mony, B. M., Mehta, M., Jarori, G. K., and Sharma, S. (2009) Plant-like phosphofructokinase from *Plasmodium falciparum* belongs to a novel class of ATP-dependent enzymes. *Int. J. Parasitol.* **39**, 1441–1453
 27. Mehta, M., Sonawat, H. M., and Sharma, S. (2006) Glycolysis in *Plasmodium falciparum* results in modulation of host enzyme activities. *J. Vector Borne Dis.* **43**, 95–103
 28. Muralidharan, V., Oksman, A., Iwamoto, M., Wandless, T. J., and Goldberg, D. E. (2011) Asparagine repeat function in a *Plasmodium falciparum* protein assessed via a regulatable fluorescent affinity tag. *Proc. Natl. Acad. Sci.* **108**, 4411–4416
 29. Pei, Y., Miller, J. L., Lindner, S. E., Vaughan, A. M., Torii, M., and Kappe, S. H. (2013) *Plasmodium yoelii* inhibitor of cysteine proteases is exported to exomembrane structures and interacts with yoelipain-2 during asexual blood-stage development. *Cell. Microbiol.* **15**, 1508–1526
 30. Sievers, F., Wilm, A., Dineen, D., Gibson, T. J., Karplus, K., Li, W., Lopez, R., McWilliam, H., Remmert, M., Söding, J., Thompson, J. D., Higgins, D. G. (2011) Fast, scalable generation of high-quality protein multiple sequence alignments using Clustal Omega. *Mol. Sys. Biol.* **7**, 539
 31. Smialowski, P., Doose, G., Torkler, P., Kaufmann, S., and Frishman, D. (2012) Proso II—a new method for protein solubility prediction. *FEBS J.* **279**, 2192–2200
 32. Michaelis, L. and Menten, M. (1913) Die kinetik der invertinwirkung. *Biochem Z* **49**, 333–369.
 33. Godiska, R., Mead, D., Dhodda, V., Wu, C., Hochstein, R., Karsi, A., Usdin, K., Entezam, A., and Ravin, N. (2009) Linear plasmid vector for cloning of repetitive or unstable sequences in *Escherichia coli*. *Nucleic Acids Res.* **38**, e88
 34. Janse, C. J., Ramesar, J., and Waters, A. P. (2006) High-efficiency transfection and drug selection of genetically transformed blood stages of the rodent malaria parasite *Plasmodium berghei*. *Nat. Protocols* **1**, 346

FOOTNOTES

Abbreviations: HADSF - Haloacid dehalogenase superfamily, PGP - phosphoglycolate phosphatase, pNPP - para-nitrophenylphosphate, RFA - regulatable fluorescent affinity

TABLES

Table 1: Kinetic parameters of *P. berghei* PGP compared with that of homologs from yeast and mouse.

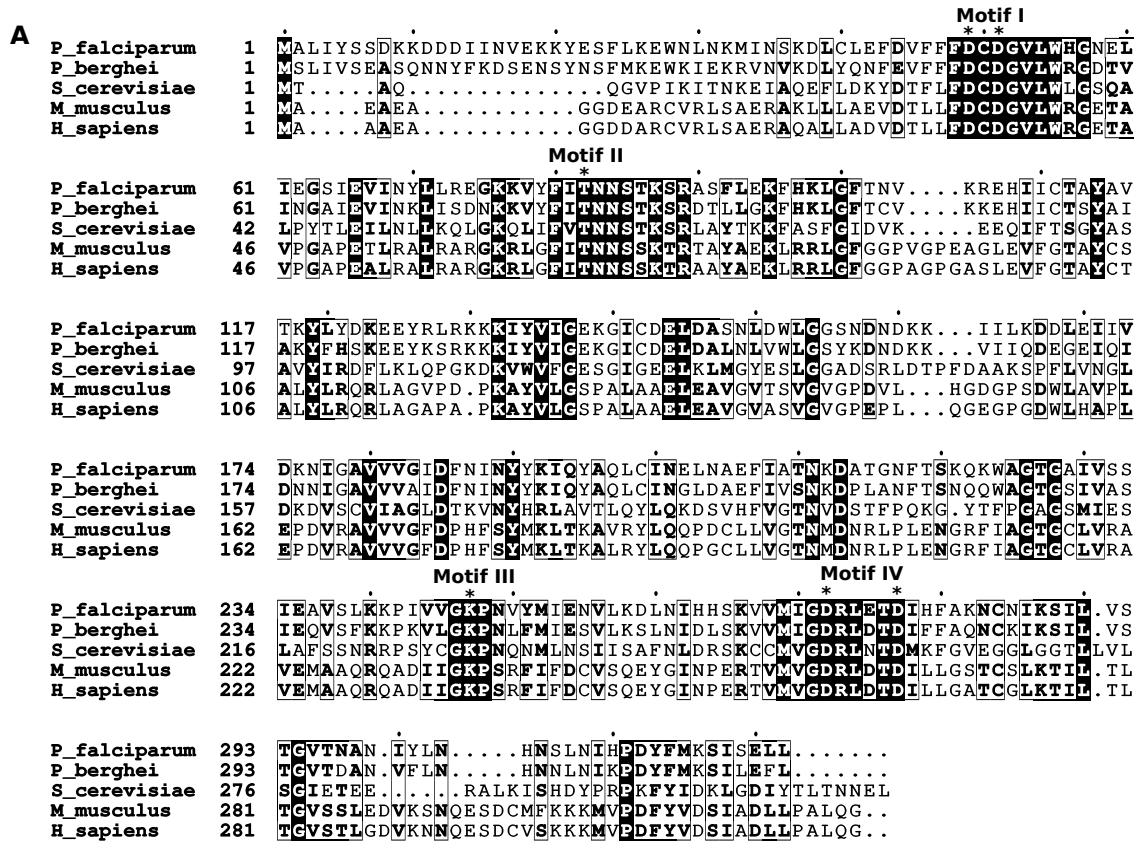
Substrate	Kinetic parameters of PbPGP			
	K_m (μM)	V_{max} ($\mu\text{mol min}^{-1} \text{mg}^{-1}$)	k_{cat} (s^{-1})	k_{cat}/K_m ($\text{M}^{-1} \text{s}^{-1}$)
β - glycerophosphate	2110 \pm 11	16.2 \pm 0.14	10.18 \pm 0.08	4827
2 - phosphoglycolate	2526 \pm 494	119.5 \pm 12.5	75.15 \pm 7.86	29747
2 - phospho L - lactate	4773 \pm 574	107 \pm 13.2	67.34 \pm 8.31	14108
Kinetic parameters of Murine PGP #				
2 - phosphoglycolate	766 \pm 68	11.34 *	6.56 \pm 0.44	8564
2 - phospho L - lactate	174 \pm 55	3.14 *	1.82 \pm 0.34	10480
Kinetic parameters of <i>S. cerevisiae</i> Pho13 #				
2 - phosphoglycolate	221 \pm 13	32.87 *	19.0 \pm 0.44	85700
2 - phospho L - lactate	747 \pm 135	13.09 *	7.57 \pm 1.04	10113

Data represents mean \pm S.E.M (N=2)

#Values taken from Collard *et al.*, 2016

* V_{max} was calculated using k_{cat} values from Collard *et al.*, 2016. Molecular mass values of 34540.68 Da and 34624.58 Da for murine PGP and Pho13, respectively was used in the calculation.

FIGURES



B

Organism	<i>P. falciparum</i>	<i>P. berghei</i>	<i>S. cerevisiae</i>	<i>M. musculus</i>	<i>H. sapiens</i>
<i>P. falciparum</i>	100	69.57	28.62	31.25	30.59
<i>P. berghei</i>	69.57	100	27.42	30.03	28.71
<i>S. cerevisiae</i>	28.62	27.42	100	31.8	32.46
<i>M. musculus</i>	31.25	30.03	31.8	100	90.65
<i>H. sapiens</i>	30.59	28.71	32.46	90.65	100

Figure 1: Multiple sequence alignment of phosphoglycolate phosphatase protein sequences. (A) Clustal omega alignment of phosphoglycolate phosphatase from *Plasmodium falciparum* (*P_falciparum*), *Plasmodium berghei* (*P_berghei*), *Saccharomyces cerevisiae* (*S_cerevisiae*), *Mus musculus* (*M_musculus*) and human (*H_sapiens*). Residues of the conserved HAD motifs involved in catalysis are indicated by *. (B) Percentage identity matrix showing the extent of homology between the sequences.

Downloaded from <http://www.jbc.org/> by guest on January 30, 2019

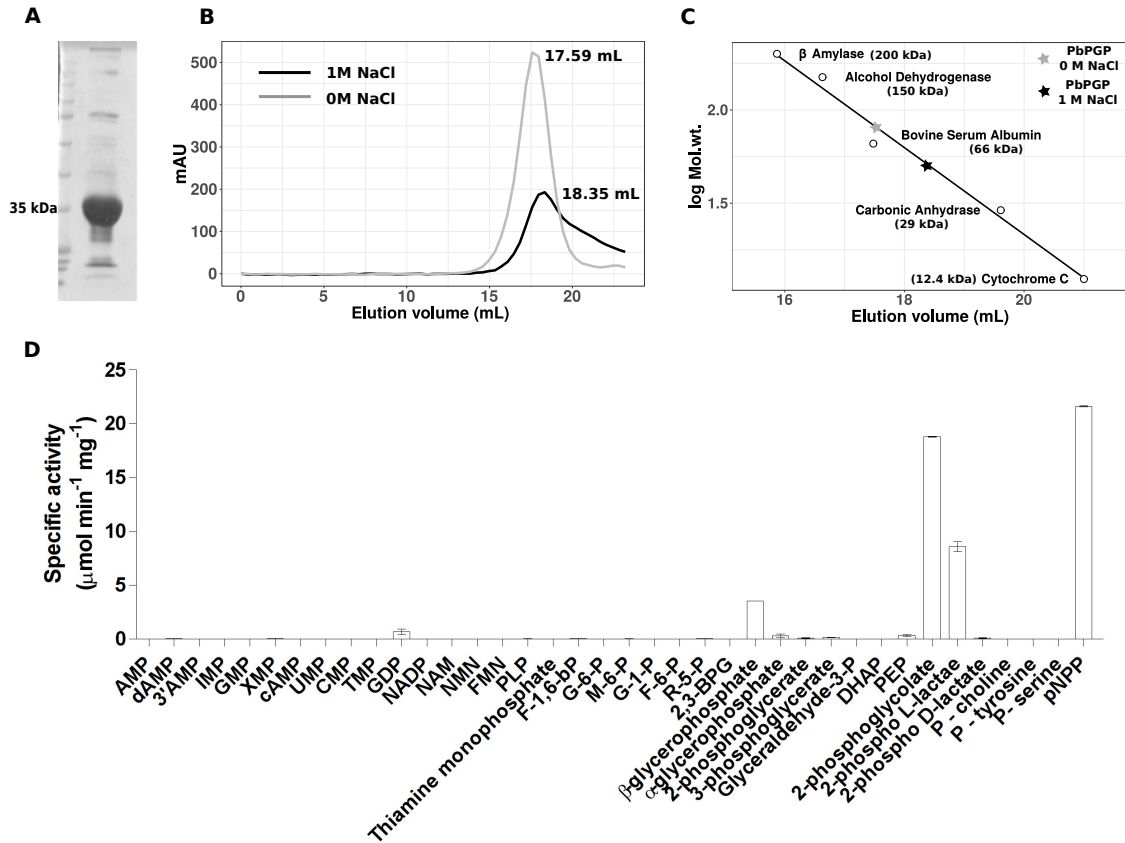


Figure 2: Purification and identification of physiological substrate of PbPGP. (A) SDS-PAGE of PbPGP purified using Ni-NTA affinity followed by size-exclusion chromatography. (B and C) Determination of oligomeric state of PbPGP. (B) Elution profile of PbPGP in the presence and absence of 1 M NaCl and (C) molecular mass calibration curve with elution volumes of PbPGP in the absence and presence of NaCl interpolated. (D) Screen for potential substrates of PbPGP. Mean specific activity values are provided for each substrate and error bars represent SD (n=2). AMP, adenosine 5' monophosphate; dAMP, deoxy adenosine 5' monophosphate; 3'AMP, adenosine 3' monophosphate; IMP, inosine 5' monophosphate; GMP, guanosine 5' monophosphate; XMP, xanthosine 5' monophosphate; cAMP, 3' 5' cyclic AMP; UMP, uridine 5' monophosphate; CMP, cytidine 5' monophosphate; TMP, thymidine 5' monophosphate; GDP, guanosine diphosphate; NADP, nicotinamide adenine dinucleotide phosphate; NAM, nicotinic acid mononucleotide; NMN, nicotinamide mononucleotide; FMN, flavin mononucleotide; F-1,6-bp, fructose 1,6-bisphosphate; G-6-P, glucose 6-phosphate; M-6-P, mannose 6-phosphate; G-1-P, glucose 1-phosphate; F-6-P, fructose 6-phosphate; R-5-P, ribose 5-phosphate; 2,3-BPG, 2,3-bisphosphoglycerate; DHAP, dihydroxyacetone phosphate; PEP, phosphoenolpyruvate.

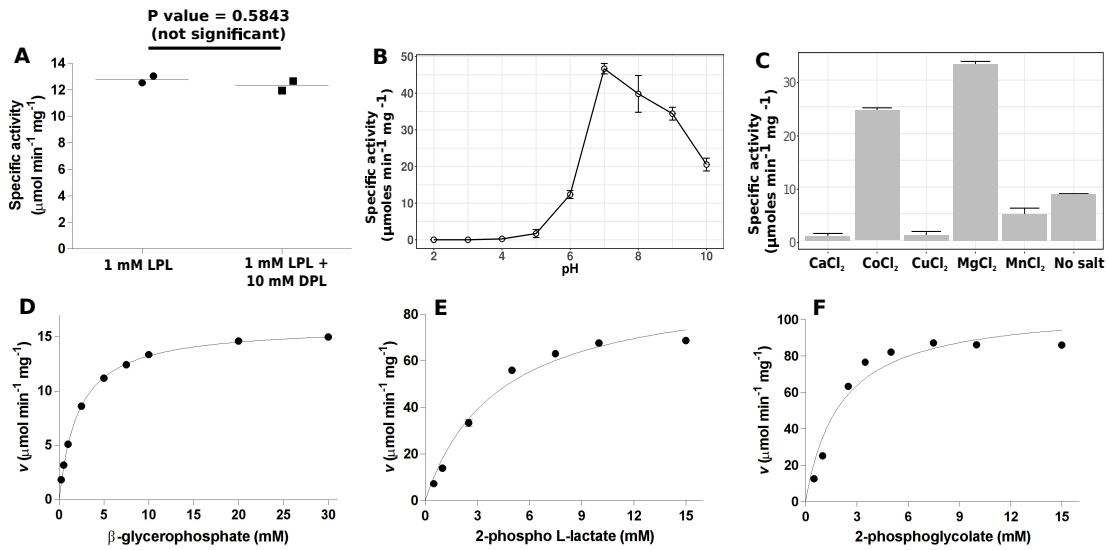


Figure 3: Biochemical and kinetic characterization of PbPGP

(A) PbPGP assay performed using 1 mM 2-phospho L-lactate (LPL) as substrate with and without 10 mM 2-phospho D-lactate (DPL). The assay conditions used were 5 mM MgCl₂, 200 mM Tricine-NaOH, pH 7.4, in a total volume of 100 μL , and at 37 °C. The reaction was initiated with 1.89 μg of enzyme and incubated for 2 minutes. Horizontal bars represent mean and circles and squares represent individual data points.

Statistical analysis was done using paired t-test. (B) pH optimum of PbPGP. (C) Histogram showing activity of PbPGP in the presence of salts of various divalent cations using pNPP as substrate. (D-F) Substrate concentration vs. specific activity plots fit to Michaelis–Menten equation for β -glycerophosphate, 2-phospho L-lactate and 2-phosphoglycolate. Substrate titration experiment was conducted in two technical replicates containing two biological replicates each. Plots from one technical replicate are shown. Each data point represents mean specific activity value and error bars represent SD (n=2).

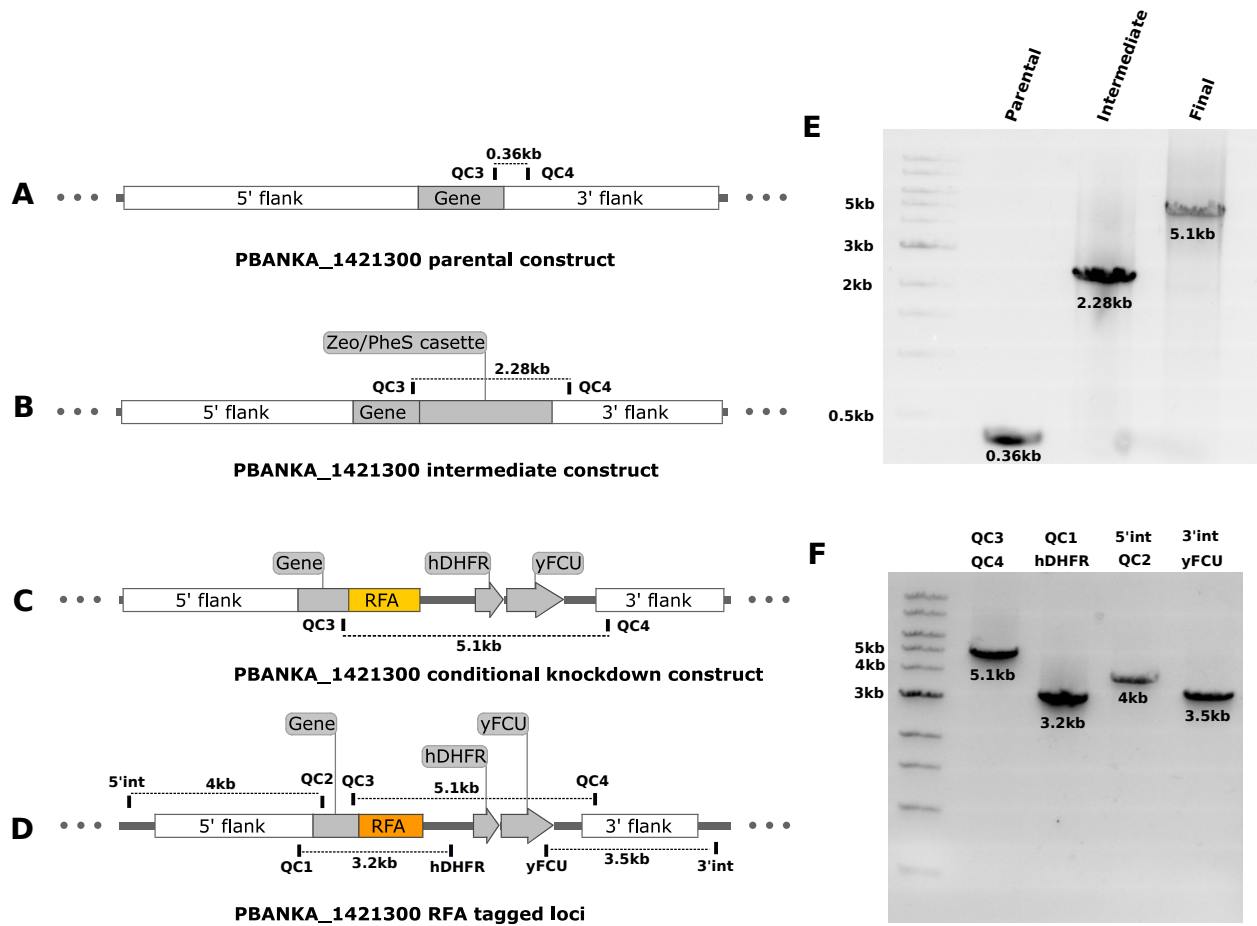


Figure 4: Generation of PbPGP conditional knockdown construct and parasite (A-D) Schematic representation of PbPGP parental, intermediate and final RFA tagging constructs and PbPGP loci after integration. Oligonucleotide primers are indicated by vertical bars and expected PCR-product size is represented by line between specific primer pairs. (E) PCR confirmation of parental, intermediate and final RFA-tagging construct. (F) Genotyping of the strain for integration of cassette in the correct loci. Primer pairs used are mentioned on top of the panel.

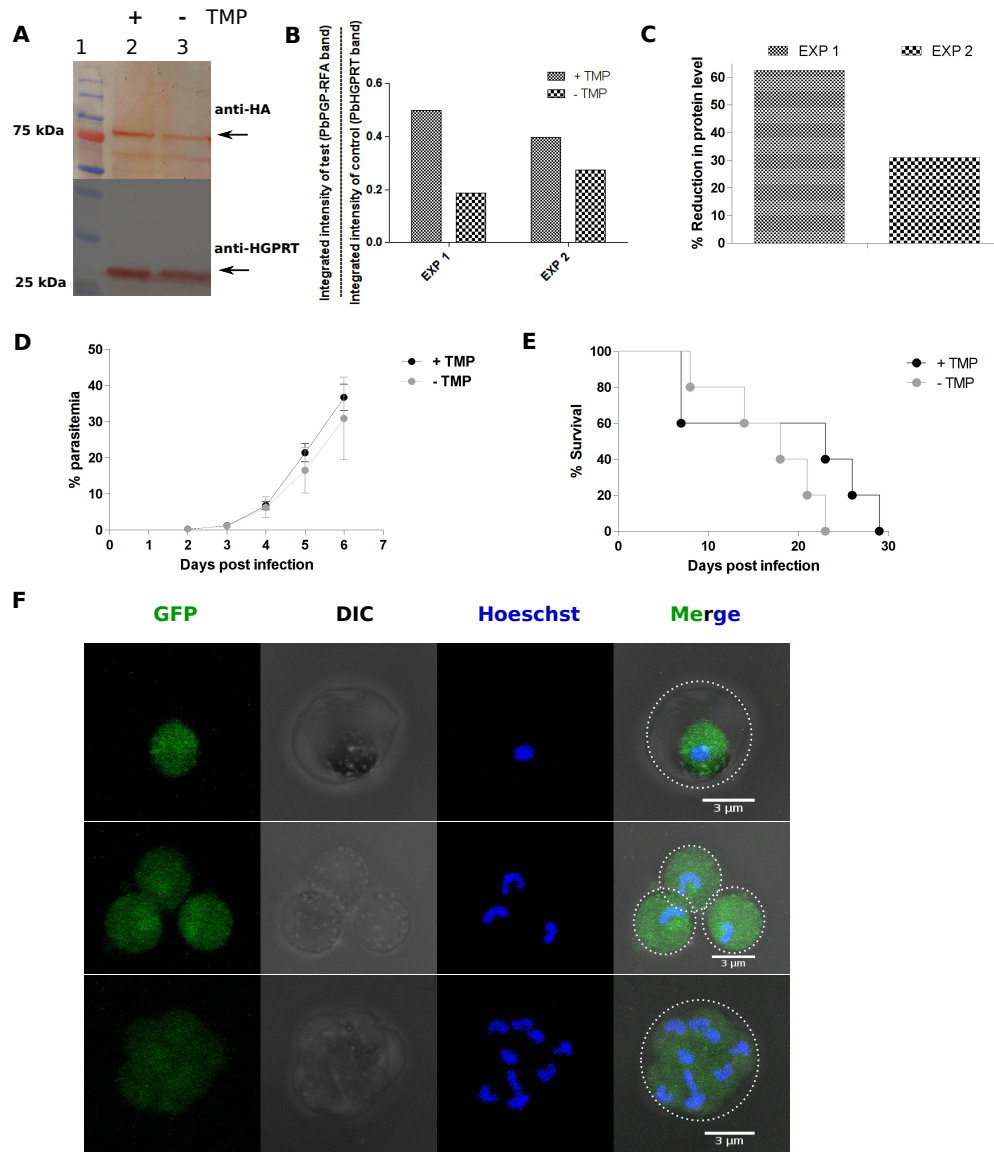


Figure 5: Phenotypic characterization of PbPGP conditional knockdown parasites and localization of PbPGP (A) Western blot analysis of cell lysates of RFA-tagged parasites from mice fed with/without trimethoprim (TMP) (30 mg in 100 mL) for 6 days. The experiment was performed twice (Exp1 and Exp2) and blot from one experimental replicate is shown. Top panel is the blot probed with anti-HA antibody and the arrow mark indicates the RFA tagged PbPGP protein. The bottom panel was probed with anti-PfHGPRT antibody. (B) Ratio of the intensity of RFA tagged PbPGP to the intensity of control HGPRT. (C) Reduction in PbPGP levels upon removal of TMP relative to the levels in the presence of TMP. Protein levels under ‘+ TMP’ condition was taken as 100%. (D) Comparison of growth rates of PbPGP conditional knockdown *P. berghei* parasites grown in mice fed with or without trimethoprim (TMP). The data represents mean \pm s.d. values obtained from five mice each infected with 1.7×10^5 parasites. Statistical analysis was done using paired t-test using Graph pad Prism V5 (P value = 0.1560, not significant). (E) Percentage survival of mice (n=5) infected with PbPGP RFA-tagged *P. berghei* parasites and fed with or without trimethoprim. The survival curves were found to be not significantly different according to Log-rank (Mantel-cox) test (P value = 0.2765) and Gehan-Breslow-Wilcoxon test (P value = 0.6740).(F) Localization of PbPGP in PbPGP RFA-tagged parasites grown in ‘+ TMP’ condition. The erythrocyte boundary is indicated by white dotted line in the merge panel.

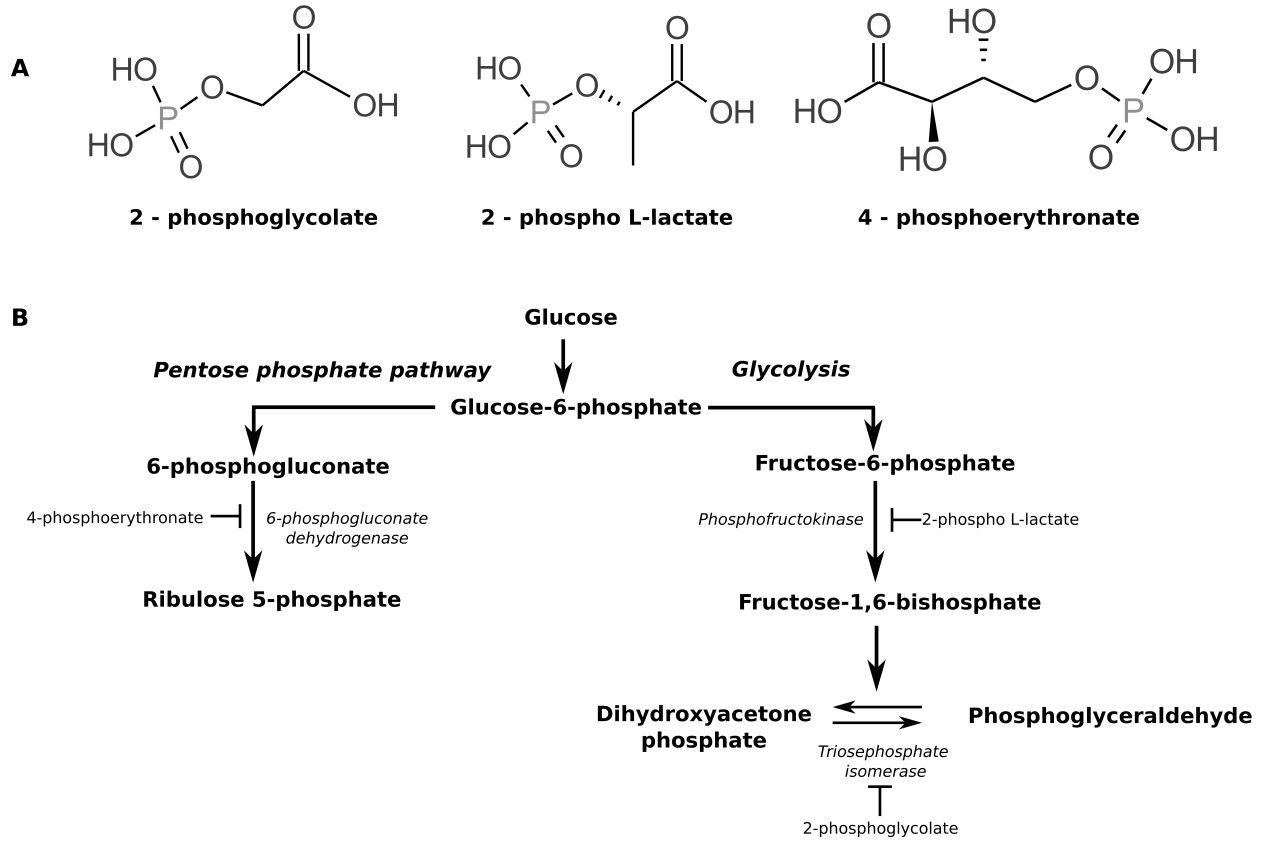


Figure 6: Metabolites that are substrates for phosphoglycolate phosphatase (A) and their inhibition of key metabolic pathways (B).

Phosphoglycolate phosphatase is a metabolic proof-reading enzyme essential for cellular function in *Plasmodium berghei*

Lakshmeesha Kempaiah Nagappa, Pardhasaradhi Satha, Thimmaiah Govindaraju and Hemalatha Balaram

J. Biol. Chem. published online January 30, 2019

Access the most updated version of this article at doi: [10.1074/jbc.AC118.007143](https://doi.org/10.1074/jbc.AC118.007143)

Alerts:

- [When this article is cited](#)
- [When a correction for this article is posted](#)

[Click here](#) to choose from all of JBC's e-mail alerts